2000-01-3500

External Flow Analysis of a Truck for Drag Reduction

Subrata Roy[1] and Pradeep Srinivasan[2]
[1]Assistant Professor, E-mail: sroy@kettering.edu
[2]Graduate Research Assistant, E-mail: pradeep@altair.com
Kettering University, Flint, MI 48504-4898

ABSTRACT

Aerodynamics of trucks and other high sided vehicles is of significant interest in reducing road side accidents due to wind loading and in improving fuel economy. Recognizing the limitations of conventional wind tunnel testing, considerable efforts have been invested in the last decade to study vehicle aerodynamics computationally. In this paper, a three-dimensional near field flow analysis has been performed for axial and cross wind loading to understand the airflow characteristics surrounding a truck-like bluff body. Results provide associated drag for the truck geometry including the exterior rearview mirror. Modifying truck geometry can reduce drag, improving fuel economy.

INTRODUCTION

Aerodynamics of trucks and other high sided vehicles is of significant interest in reducing road side accidents due to wind loading and in improving the fuel economy [1-3]. Conventional Aerodynamic development of trucks is carried out by wind tunnel testing of a miniature model with the working floor representing the road. Recognizing limitations of the wind tunnel boundary conditions, considerable efforts were made in the last decade to study vehicle aerodynamics computationally. These efforts range from studying the window profile of the vehicle [4] to drag implications of truck mirrors [5].

Takeuchi and Kohri [6] describe a method for predicting aerodynamic drag and engine cooling performance for trucks and buses using CFD. In particular, an adequate method was developed to accurately obtain the wake flow behind the body. Wake Flow is a dominant component of the total drag.

In this paper, a three-dimensional near field flow analysis has been performed to understand the airflow characteristics surrounding a truck-like bluff body. The unsteady flow distribution is calculated by solving the Navier-Stokes equation with a two-equation (*k-e*) turbulence closure model. Results provide boundary layer details and associated drag for the truck geometry. Drag can be reduced by modifying the truck geometry, hence improving fuel economy. The paper also documents a comparison of the axial and cross wind load for a vehicle moving at 60 mph.

THEORETICAL DEVELOPMENT

The computational technique utilized in this paper involves analysis of two computational components sequentially. First, computational fluid dynamics (CFD) is used to analyze the three-dimensional flow structure and calculate the pressure distribution on the truck's external surface. Then, resulting drag coefficients are utilized to compute flow drag and estimate fuel consumption.

COMPUTATIONAL FLUID DYNAMICS

As direct Navier-Stokes (DNS) solutions remain impractical for industrial problems, the technical framework requires solving the compressible Navier-Stokes (CNS) equation with some turbulence closure model. In this paper, the effect of turbulence is simulated with a two equation k-ε model.

CNS-ALE Formulation

To accurately describe the moving boundaries, physical quantities are described at fixed points in space in the Eulerian description and specific material particles are followed using the Lagrangian description. In this case, each point in space has a material velocity **u** and a grid velocity **w** describing its arbitrary movement. In this context, classical CNS conservation laws are written as:

Mass: $\partial\rho/\partial t + [(\mathbf{u}-\mathbf{w})\bullet\nabla]\rho + \rho\nabla\bullet\mathbf{u} = 0$ (1a)
Momentum: $\partial\mathbf{u}/\partial t + [(\mathbf{u}-\mathbf{w})\bullet\nabla]\mathbf{u} - \nabla\bullet\underline{\boldsymbol{\sigma}}/\rho = 0$ (1b)
Energy: $\partial\rho e/\partial t + [(\mathbf{u}-\mathbf{w})\bullet\nabla]\,\rho e + (\rho e+p)\nabla\bullet\mathbf{u} = 0$ (1c)

In Equation (1), ρ is fluid density, **u** is the fluid velocity, e is the specific energy and $\underline{\boldsymbol{\sigma}}$ is the stress tensor. Note that for **u**=**w**, Equations (1a)-(1c) reduces to a Lagrangian formulation, while **w**=0 describes the Eulerian case. A single formulation is thus able to describe the evolution of physical variables in the laboratory reference frame and in a grid with any arbitrary movement (e.g. rotation). The coupling between the rotating grid and the fixed grid may be done using a simple finite element interpolation scheme. In this paper, **w** was set to zero for a fixed grid.

Turbulence Modeling

This model introduces two equations, one for the turbulent kinetic energy *k* and the other for its dissipation rate *e*. These equations are included in the set of the transformed equations for (1a-c). The effect of this model is to introduce an additional viscosity, called turbulent viscosity, which is calculated as a function of density *r* in Equation (2).

$$m_t = C_m r \frac{k^2}{e} \tag{2}$$

The turbulent viscosity is not a fluid property, but rather a property of the flow field. Its value is added to the molecular viscosity and yields an effective viscosity, m_{eff}, which is used in the calculations. The various terms associated with the *k-e* model are the production of turbulence *G*, some arbitrary constants C_i, and the effective transport coefficient G_{eff}. The latter is equal to the effective viscosity m_{eff} for the momentum equations, which for the *k*- and *e*–equations, is equal to m_{eff}/Pr_t , where Pr_t is the respective turbulent Prandtl number. The generation of turbulence is calculated from the following equation:

$$G = m_t\left(\frac{\partial u_i}{\partial x_k}\frac{\partial x_k}{\partial x_j} + \frac{\partial u_j}{\partial x_k}\frac{\partial x_k}{\partial x_i}\right)\frac{\partial u_i}{\partial x_k}\frac{\partial x_k}{\partial x_j}. \tag{3}$$

In Equation (3), x_i is the transformed coordinate system. The *k* and *e* at the inlet are calculated from the following expressions:

$$k_{in} = \frac{3}{2}(T_u \cdot u)^2 \quad e_{in} = \frac{k_{in}^{3/2}}{L_e} \tag{4}$$

where T_u is the turbulence level, which is chosen equal to the 10%. L_e is a characteristic length of the domain.

Solution Procedure

Equations (1) – (3) constitute a system of non-linear algebraic equations. The system is linearized by relaxation. A streamline upwinding technique is employed for stabilizing numerical iterations. The pressure corrections are used to correct the pressure and the velocities. This predictor-corrector procedure constitutes an iteration. The solution is declared convergent when the maximum residual for each of the state variables becomes smaller than a convergence criterion of 10^{-4}. Here, the convergence of a solution state vector $\mathbf{V}\subset\mathbf{q}$ (where **q** is the unknown vector) on node *n* is defined as the norm:

$$\frac{\|\mathbf{V}_n - \mathbf{V}_{n-1}\|}{\|\mathbf{V}_n\|} \le 10^{-4} \tag{5}$$

FLOW DRAG AND FUEL CONSUMPTION

As in the case of cars and light trucks, flow drag should be an important design criterion for heavy vehicles. According to [1] (see p.416), the power required by a high-bodied, 40-ton Tractor Trailer to overcome air drag is 18 kW at 37 mph (50km/h) and 40 kW at 50 mph (80 km/h). However, unlike a car, the shape of a commercial truck is driven by cargo space. Statutory size limits impose restrictions on the aerodynamic design of the load-carrying rear section of the vehicle. The front end remains an open design location for flow drag minimization and thus reduction in fuel consumption.

Drag vs fuel consumption

The drag force F_D is given by the air density ρ, relative velocity V, drag coefficient C_D and the surface area A:

$$F_D = C_D \frac{ArV^2}{2} \tag{6}$$

Based on a typical frontal area *A* of 4.5 m^2 and a coefficient of drag C_D of 0.7, Cresswell & Hurtz [5] documented that the contribution of three different mirror shapes to drag ranges from 5.3% (M1) to 10% (M3) of the total frontal aerodynamic drag of the truck. The effect of different frontal design on C_D is well documented in Figure 1. Figure 1a shows the relationship of the flow drag coefficient to the Reynolds number. In figure 1b, the change in drag coefficient due to the shape of the frontal section of the truck is compared for six different designs.. The yaw angle, independent variable in Figure 1c is defined as the relative angle between the truck velocity and the resultant velocity of crosswind and truck.

The fuel consumption (L) for a gasoline powered truck is given in [5] as:

$$\frac{L}{100} = 0.01264 \times F_D \tag{7a}$$

while for a diesel-engine powered truck it is,

$$\frac{L}{100} = 0.008051 \times F_D \tag{7b}$$

Considering a 35% power train efficiency for a diesel engine, estimates in [5] indicate 800 litres/yr fuel savings between the M1 and M3 mirror, for 150,000 km annual highway driving. Fuel savings estimated for a 25% power train efficiency for a gasoline fueled truck under similar considerations is 1250 litres.

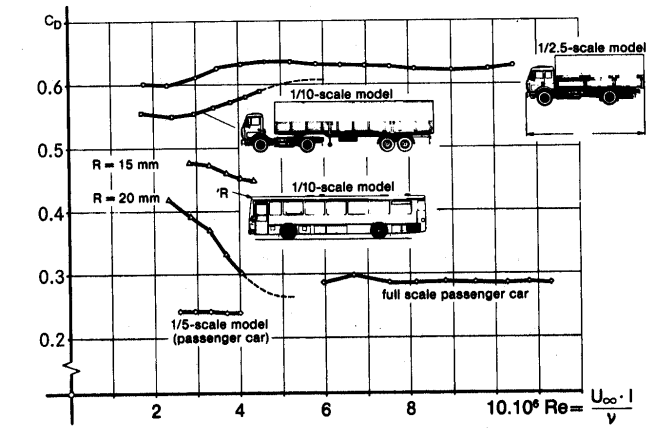

(a)

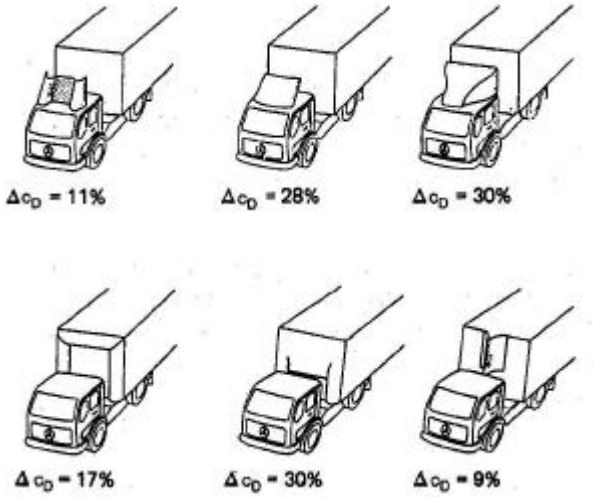

(b)

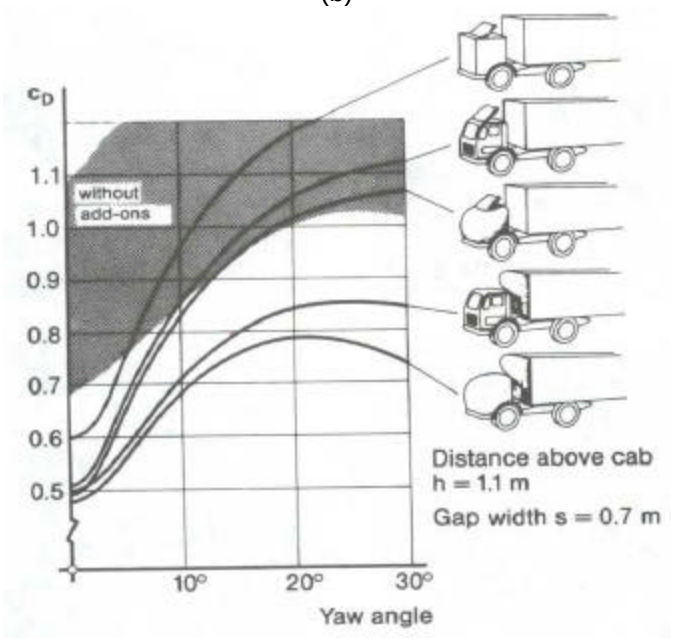

(c)

Figure 1. Effect of shape of the truck on the drag coefficient [1].

NUMERICAL RESULTS

Two different truck shapes were modeled. For these shapes flow drag and fuel estimations were computed for two different boundary conditions, namely, no crosswind and moderate crosswind. Table 1 shows the simulated cases documented in this paper. Here onwards, the baseline truck front design will be referred to as A and the modified design as B (see Figure 2 below).

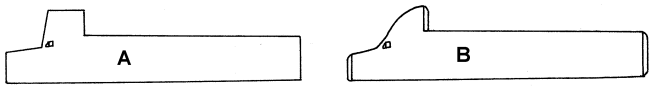

Figure 2. Truck designs A and B used for simulation.

Boundary Conditions

The truck is placed at the center of a road that is 40l x 10d, where l is the length of the truck and d is the maximum width. On the road and on the truck exterior typical wall boundary conditions are applied, i.e., the no-slip condition for the velocities and the wall functions for the *k* and *e*. The coordinates are selected such that *x* and u are along the truck length, *y* and v are vertical to the road, and *z* and w are along the width of the truck. At the inlet a geometry fixed velocity profile is prescribed, and then this is decomposed into u- and w- profiles; the v-profile assumes zero values. For cases with no crosswind (A1 and B1 in Table 1), the u-velocity is prescribed a non-zero value in the upstream boundary, while the v and w components are set equal to zero. The *k* and *e* are calculated from (4). For cases A2 and B2, the crosswind w is applied in the z direction. Finally, the far-field pressure boundary condition is applied on other boundaries. The freestream and downstream conditions are zero gradients for all state variables.

Simulation results

Results of CFD simulations done on a SUN Ultra60 machine are documented in Figures 3-7. The domain is discretized into 1,780,000 finite tetrahedral elements. A typical simulation for both cases A and B took about 8 cpu hours to converge. Corresponding computed drag and estimated fuel consumption normalized by results from baseline truck A1 are shown in Table 1.

Table 1. Comparison of cases documented without considering the tire rolling resistance.

Simulation	Cases			
	A1	A2	B1	B2
Truck speed (mph)	60	60	60	60
Crosswind (mph)	0	30	0	30
Computed drag	1	1.26	0.67	0.85
Estimated fuel (L/100)	1	1.35	0.59	0.78

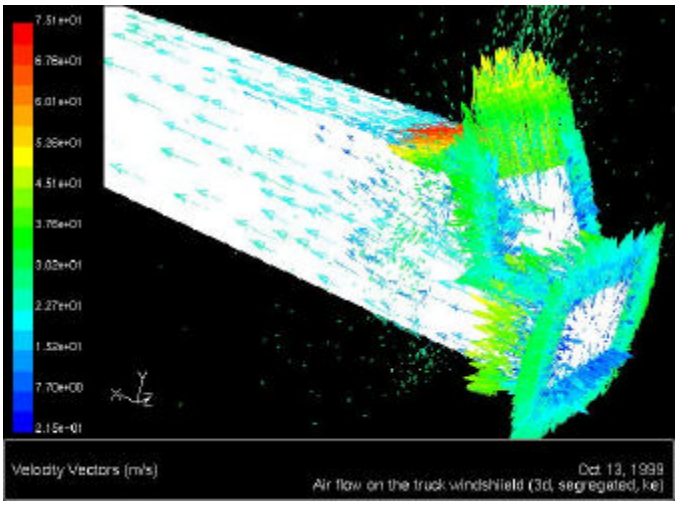

Figure 3a. The velocity vectors for truck A plotted on the vehicle surface and colored by speed shows areas of high velocity gradients and pressure changes.

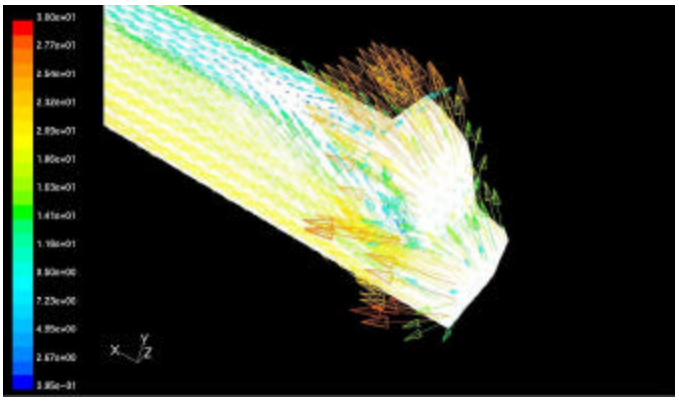

Figure 3b. Improvement in velocity vectors near the truck front is seen for truck B.

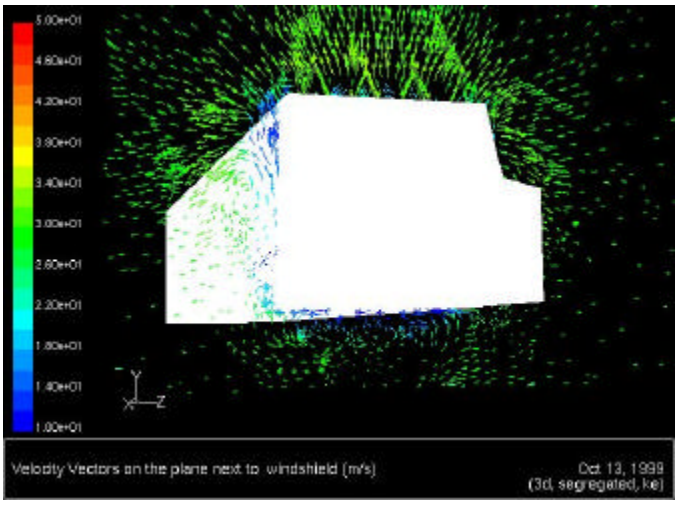

Figure 4a. Velocity vectors for truck A on the vertical plane near the exterior rearview mirror shows the three-dimensional vortices in the spanwise direction.

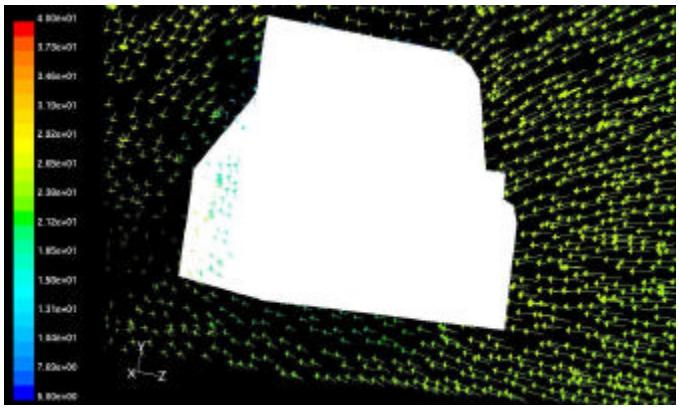

Figure 4b. Reduced vortices near the exterior mirror for the modified truck B.

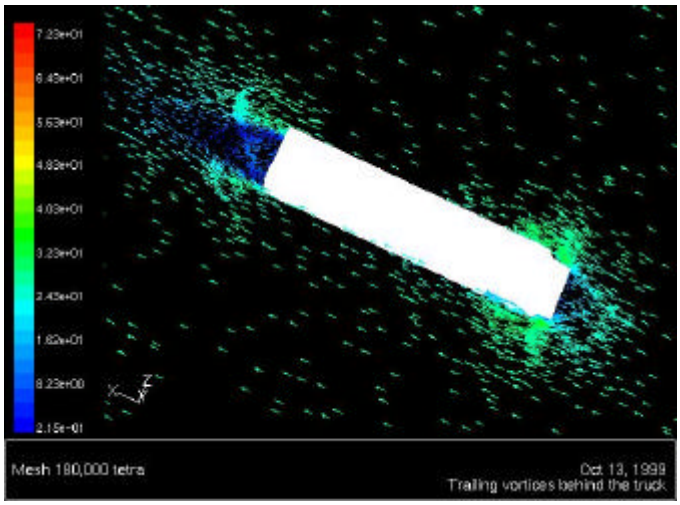

Figure 5. General trend of flow vectors along the truck in a horizontal plane cut in the mid-height of the truck.

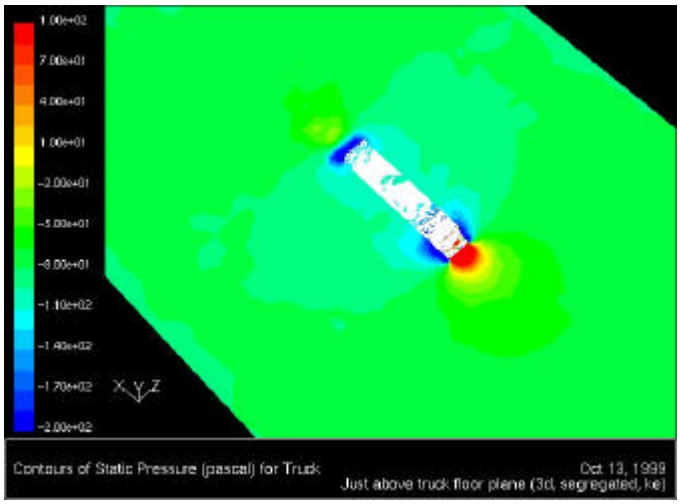

Figure 6a. Corresponding static pressure contours along the truck A in a horizontal plane cut in the mid-height of the truck shows dominant areas causing flow drag.

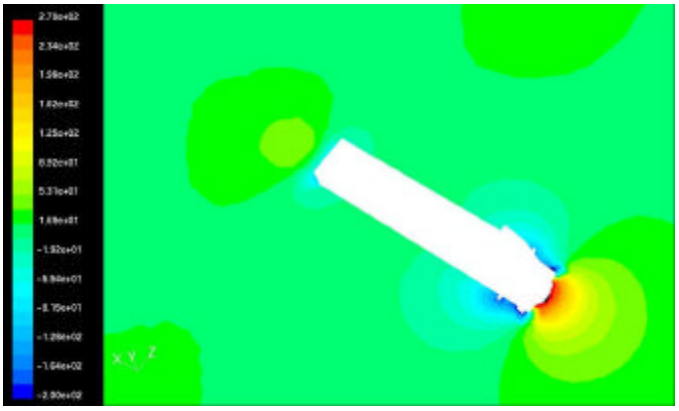

Figure 6b. Modified geometry B has reduced drag as shown in reduced dark patches (as compared to Figure 5a) surrounding the truck.

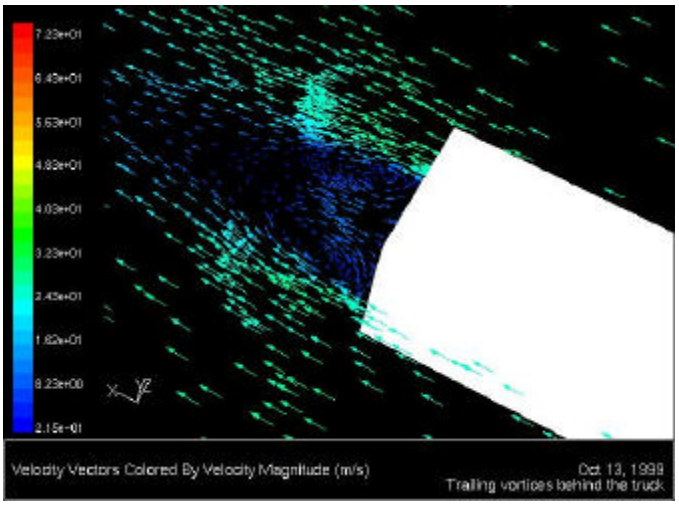

Figure 7a. Details of flow vectors behind the truck A on a horizontal plane shows strong recirculation and resultant source of pressure drop.

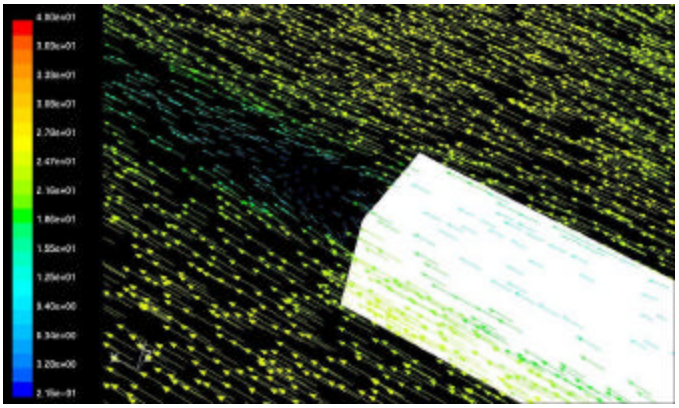

Figure 7b. Less flow vortices behind the truck B.

CONCLUSION

A fully three-dimensional near field flow analysis has been performed to understand the airflow characteristics surrounding the truck-like bluff body. The unsteady flow distribution is calculated by solving the Navier-Stokes equation with a two-equation (*k-e*) turbulence closure model. Results provide boundary layer details and associated drag for the truck geometry. The analyses utilized 1.78 million finite elements and included the rearview mirror. Results involving a crosswind of 30 mph shows that for an improved aerodynamic design B over 30% drag reduction is achieved as compared to design A. Corresponding estimated fuel savings is nearly 35%. These results confirm that modifying the truck geometry can significantly improve fuel efficiency. More work should be done on practical truck geometry so that the results can be commercially useful.

REFERENCES

1. H. Götz and G. Mayr, Aerodynamics of Road Vehicles (Ed. W.H. Hucho), SAE International, pp. 415-488, 1998.
2. Topics in vehicle aerodynamics, SP-1232, SAE International, 246p, 1997.
3. S.A. Coleman and C.J. Baker, Reduction of accident risk for high sided road vehicles in cross winds, Journal of Wind Engineering and Industrial Aerodynamics, Vol. 44, pp. 2685-2695, 1992.
4. V. Eowsakul and T.J. Ortolani, Improving the aerodynamic characteristics of a Dodge Ram pickup truck, ASME IMECE Paper No. 97-WA/DE-18, 8p, 1997.
5. M.G.L. Cresswell and P.B. Hertz, Aerodynamic drag implications of exterior truck mirrors, SAE Technical Paper Series, No. 920202, pp. 29-34, 1992.
6. T. Takeuchi and I. Kohri, Development of truck and bus aerodynamics using computational fluid dynamics, JSAE Review, Vol. 18(2), p.188, 1997.

CONTACT

Subrata Roy was born in India where he did his undergraduate schooling in Mechanical Engineering at Jadavpur University, Calcutta. He earned his MS and PhD in Engineering Science from University of Tennessee, Knoxville, with specialization in Computational Fluid Dynamics. Roy then worked as a technical consultant for Boeing, the US Army and Allied Signal. He pioneered the flow induced noise technology at Case (new name CNH) Corporation where he served as a technical specialist. Currently he is an Assistant Professor of Mechanical Engineering department at Kettering University. He has published numerous technical papers and a book on popular science. In summer 2000, Roy received NASA/OAI Collaborative Research Fellowship for his work in computational magnetoplasmadynamics.
Web: http://www.kettering.edu/~sroy.